

Magnetospheric Multiscale Overview and Science Objectives

J.L. Burch¹ · T.E. Moore² · R.B. Torbert³ · B.L. Giles²

Received: 20 March 2015 / Accepted: 12 May 2015 / Published online: 30 May 2015
© The Author(s) 2015. This article is published with open access at Springerlink.com

Abstract Magnetospheric Multiscale (MMS), a NASA four-spacecraft constellation mission launched on March 12, 2015, will investigate magnetic reconnection in the boundary regions of the Earth's magnetosphere, particularly along its dayside boundary with the solar wind and the neutral sheet in the magnetic tail. The most important goal of MMS is to conduct a definitive experiment to determine what causes magnetic field lines to reconnect in a collisionless plasma. The significance of the MMS results will extend far beyond the Earth's magnetosphere because reconnection is known to occur in interplanetary space and in the solar corona where it is responsible for solar flares and the disconnection events known as coronal mass ejections. Active research is also being conducted on reconnection in the laboratory and specifically in magnetic-confinement fusion devices in which it is a limiting factor in achieving and maintaining electron temperatures high enough to initiate fusion. Finally, reconnection is proposed as the cause of numerous phenomena throughout the universe such as comet-tail disconnection events, magnetar flares, supernova ejections, and dynamics of neutron-star accretion disks. The MMS mission design is focused on answering specific questions about reconnection at the Earth's magnetosphere. The prime focus of the mission is on determining the kinetic processes occurring in the electron diffusion region that are responsible for reconnection and that determine how it is initiated; but the mission will also place that physics into the context of the broad spectrum of physical processes associated with reconnection. Connections to other disciplines such as solar physics, astrophysics, and laboratory plasma physics are expected to be made through theory and modeling as informed by the MMS results.

Keywords Magnetic reconnection · Space plasma physics

✉ J.L. Burch
jburch@swri.edu

¹ Southwest Research Institute, San Antonio, TX, USA

² NASA Goddard Space Flight Center, Greenbelt, MD, USA

³ University of New Hampshire, Durham NH and Southwest Research Institute, Durham, NH, USA

1 Introduction

In a collisionless magnetized plasma, the magnetic field tends to be “frozen” into the plasma because of high electrical conductivity. Abundant evidence exists that this frozen-in condition often breaks down. Magnetic field lines embedded in solar system and astrophysical plasmas then become interconnected, either along their own length or with magnetic fields connected to other bodies. When this interconnection (or reconnection) occurs, magnetic-field energy is converted to kinetic energy of the plasma ions and electrons, and plasmas can move directly across boundaries separating regions such as stellar winds and magnetospheres. This process occurs most efficiently when the magnetic fields in adjacent plasma domains are oriented opposite or antiparallel to one another (antiparallel reconnection) but also occurs for arbitrary configurations in which the two fields have an antiparallel component (component or guide-field reconnection).

The reconnection process, whether in collisional plasmas near stellar bodies (Galeev et al. 1979), marginally collisionless plasmas in the solar corona (Cassak and Shay 2012), or in collisionless plasmas within stellar winds and planetary magnetospheres (Phan et al. 2006; Nagai et al. 2013), is thought to be of great importance for energy transfer throughout the universe. For example, high-resolution soft X-ray images from the TRACE and Hinode satellites have confirmed that reconnection of magnetic fields in the upper atmosphere of the Sun plays a key role in producing the explosive ejection of solar material outward into the solar system (Goff et al. 2005; Doschek et al. 2014). Such eruptive events, known as coronal mass ejections or CMEs, are responsible for major magnetic storms on Earth (Webb et al. 2000). Recent observations by McKenzie (2013) have shown that at times reconnection in the solar corona occurs in plasmas with $\beta > 1$, as opposed to the low- β environment that has traditionally been considered. This observation suggests that solar reconnection may at times be more similar to reconnection in the Earth’s magnetosphere than was previously supposed. Geomagnetic disturbances occur more frequently and become stronger as the magnetic field in the solar wind (and within CMEs) becomes more southward and thus more antiparallel to the Earth’s magnetic field (Cain et al. 2000). This fact and the accelerated plasma flows observed at these times along the boundary of the Earth’s magnetic field and within its extended tail (Paschmann et al. 1979; Gosling et al. 1986) are consistent with the acceleration of charged particles that is expected to result from magnetic reconnection.

Because of the universal importance of magnetic reconnection, the NASA Solar Terrestrial Probes (STP) Program initiated a carefully crafted experiment in space. The mission, named Magnetospheric Multiscale (MMS), began with the launch of a four-spacecraft constellation on March 12, 2015. The scientific target of this mission is reconnection in the boundary regions of the Earth’s magnetosphere, particularly along its dayside interface with the solar wind (the magnetopause) and at the transition between open and closed magnetic field lines in the magnetic tail (across the neutral sheet) as shown by the boxes in Fig. 1.

Substantial evidence, both direct and indirect, exists for the occurrence of reconnection at the magnetopause and in the magnetotail and for the crucial role that it plays in the topology and dynamics of the magnetosphere. Analytical studies and numerical simulations have contributed important insights into the physics of reconnection. However, many fundamental questions remain to be answered. The MMS Science and Technology Definition Team report (Curtis 1999) identified the following outstanding scientific questions about reconnection:

1. What are the kinetic processes responsible for collisionless magnetic reconnection, and how is reconnection initiated?
2. Where does reconnection occur at the magnetopause and in the magnetotail, and what influences where it occurs?

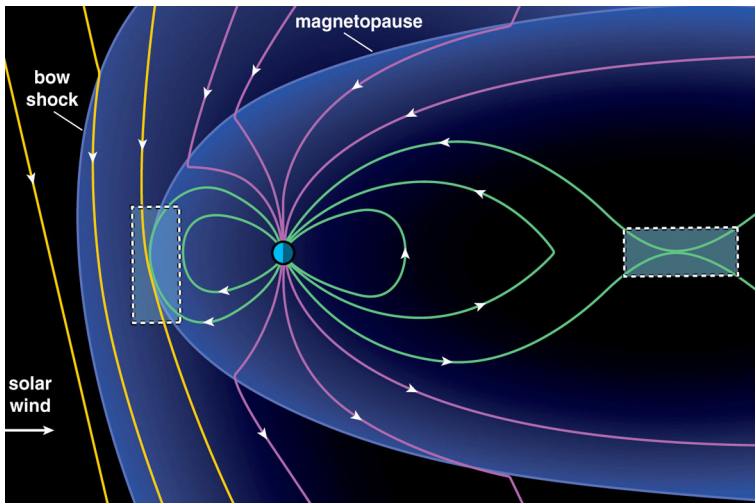


Fig. 1 Sketch of Earth's magnetosphere in noon-midnight meridian plane showing *rectangular-shaped regions* where magnetic reconnection is most often observed

3. How does reconnection vary with time, and what factors influence its temporal behavior?
4. At what rate (as a fraction of the Alfvén speed) does reconnection proceed, and how is the rate affected by ion composition, plasma or magnetic symmetry, or other factors?

Since that time significant progress has been made as a result of theory and numerical modeling (Hesse et al. 2014), laboratory investigations (Uzdensky and Kulsrud 2006), and space-based measurements (Mozer et al. 2011; Graham et al. 2014). While tremendous advances have been made with data on the MHD and ion scales (both spatial and temporal), complete answers to question 1 (about kinetic processes) will depend on carefully crafted measurements at the electron scales. For this reason the science objectives of the MMS mission have evolved to focus sharply on the electron scale with significantly higher time resolution and on closer spacecraft spacing than prescribed in the STDT report. As a result, the baseline science goal for MMS is to:

Understand the microphysics of magnetic reconnection by determining the kinetic processes occurring in the electron diffusion region that are responsible for collisionless magnetic reconnection, especially how reconnection is initiated.

In priority order, MMS will address three specific objectives:

1. Determine the role played by electron inertial effects and turbulent dissipation in driving magnetic reconnection in the electron diffusion region.
2. Determine the rate of magnetic reconnection and the parameters that control it.
3. Determine the role played by ion inertial effects in the physics of magnetic reconnection.

MMS high-resolution plasma and fields measurements acquired at multiple points in space, over a range of spatial scales and at both high and low latitudes, will make it possible to address these questions. The answers that MMS provides will ultimately reveal how the magnetosphere is driven by the solar wind and will yield a basic understanding of how, why, and with what speed reconnection proceeds in a collisionless plasma. Particularly exciting is the prospect that, owing to its high spatial resolution (~ 10 km interspacecraft separation) and unprecedented time scales (30 ms for 3D electron distribution functions), MMS will

be able to observe directly the microphysical processes that lead to the breakdown of the frozen-in-flux constraint and allow reconnection to occur.

2 Current Understanding of Magnetic Reconnection

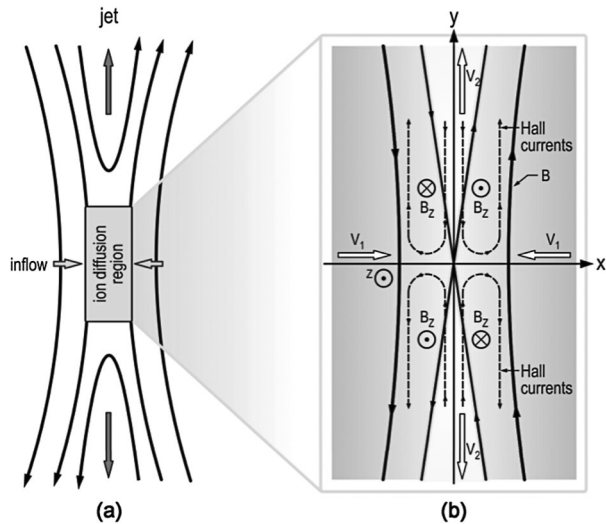
The early history of magnetic reconnection research is generally well known in the community as is summarized by Burch and Drake (2009). It began with the observations of Giovanelli (1947), while still a graduate student, that solar flares usually occurred where formation of a magnetic null was expected based on the magnetic polarities of nearby sunspots. His advisor, Sir Fred Hoyle (1949) extended this idea by suggesting that strong currents are expected at magnetic null points in the solar atmosphere and should also occur at the null points formed between the solar and geomagnetic fields, causing particle acceleration and aurora. A subsequent Hoyle graduate student, James Dungey, took up this latter idea, which led to his ground-breaking reconnection model of the magnetosphere (Dungey 1961).

Sweet (1958) reported the first attempt to explain reconnecting magnetic fields in his neutral point theory of solar flares. The theory, which was primarily based on hydrodynamics with electrical resistance effects, produced a flattening of two colliding regions with oppositely-directed magnetic fields. This flattening produced a very broad and thin layer of current, within which the magnetic fields are dissipated by electrical resistance, and very restricted regions through which reconnected magnetic fields and plasma are ejected. While this type of reconnection is observed in the laboratory (Ji et al. 1999) and is thought to occur in dense regions such as the solar photosphere and chromosphere (Litvinenko and Chae 2009), it proceeds far too slowly to explain explosive coronal phenomena such as solar flares. This problem was recognized by Parker (1957) who proposed that rapidly increasing magnetic gradients in the dissipation region would expel the plasma at a much higher rate—the Alfvén speed. This modification (Sweet-Parker reconnection) increased the speed of the reconnection process but not by enough to explain explosive phenomena because the dissipation region was still very long and thin.

The next advance was made by Petschek (1964, 1995) based on aerodynamic principles, which described a pronounced opening up of the exhaust region by the propagation of dispersive Alfvén waves leading to standing switch-off slow shocks along the boundary of the exhaust region. The result of Petschek's model was a much shorter diffusion region, which speeds up the reconnection rate drastically because the reconnected magnetic fields and entrained plasma have a much shorter distance to travel before escaping. Moreover the waves contribute to the magnetic-field annihilation much faster than resistive diffusion alone, which was assumed in the Sweet-Parker model. The current picture of the geometry of the reconnection region obtained in computer simulations and observed in space and the laboratory is in fact very close to Petschek's result. However, Petschek's description of an outflow region bounded by switch-off slow shocks, while pleasing in its simplicity, has not been borne out exactly because this type of shock is very rarely observed in space (Drake et al. 2009). However, this detail does not prevent Petschek's model from explaining most observations of reconnection geometry.

As pointed out by Parker (1957) the outflow velocity from the reconnection region is the Alfvén velocity, so the reconnection rate (as a fraction of the Alfvén velocity) is determined by the inflow velocity. As a result, the aspect ratio (length versus width) of the diffusion region provides another measure of the reconnection rate. Conservation of particles and magnetic flux dictate that longer and thinner diffusion regions, as in Sweet-Parker, will have slower inflow velocities with reconnection rates 10 to 100 times slower than required for

Fig. 2 (a) Basic reconnection geometry following (Petschek 1964). (b) Hall currents and quadrupolar magnetic field components in the ion diffusion region following (Sonnerup 1979)



solar flares. On the other hand, Petschek (1964) estimated a growth time of about 100 s, which is comparable to flare time scales. A simplified sketch of the basic Petschek geometry is shown in Fig. 2(a).

The next major breakthrough in reconnection theory was the recognition that the diffusion region is separated into an ion diffusion region and a smaller embedded electron diffusion region (e.g., Biskamp et al. 1995). As plasma and its frozen-in magnetic field move into the ion diffusion region, the electrons remain magnetized while the ions become decoupled from the magnetic field. The theory describing the resulting plasma motions is referred to as Hall-MHD because the differential motion of ions and electrons result in currents transverse to the magnetic field (as in the Hall effect in conductors and semiconductors). Sonnerup (1979) analyzed these currents and showed that they produce a quadrupolar magnetic field component directed perpendicular to the plane of reconnection. The importance of this prediction is far-reaching, partly because it produces a magnetic-field component parallel to the reconnection electric field. A field-aligned current in the same direction as the electric field would contribute to the dissipation required in the diffusion region, and may be the “smoking gun” for reconnection that experiments like those to be conducted by MMS will be seeking. Sonnerup’s prediction of the quadrupolar magnetic field component is illustrated in Fig. 2(b), which is adapted from Fig. 24 of Sonnerup (1979).

One of the enduring mysteries about reconnection is the observation of high-energy particles (100 s of keV to MeV), e.g., in the magnetotail at the initiation of substorms. As noted by Sonnerup (1979) these energies far exceed the total potential drop across the magnetotail. In addition, and also noted by Sonnerup (1979), because of the small size of the diffusion region, accelerated particles can only spend a very small length of time under the influence of the reconnection electric field. The conclusion often reached is that phenomena such as fluctuating reconnection electric fields or induced electric fields produced by changes in the magnetic field caused by reconnection could be responsible for the high particle energies. For this reason it is important that energetic particle measurements be made inside the diffusion region with appropriately high time resolution (Mauk et al. 2014).

Comparison of measurements from Polar with particle-in-cell simulations of asymmetric reconnection with a guide field at the dayside magnetopause by Mozer and Pritchett (2009) show that the electron dissipation regions with their associated parallel electric fields

and currents are not confined to the region immediately surrounding the X-line but extend well into the reconnection separatrix and exhaust regions. If similar extensions occur in the mainly symmetric reconnection of the magnetotail then they could be important for generation of the reconnection fronts observed by Angelopoulos et al. (2013). These recent observations suggest a larger target for MMS as well as different reconnection and dissipation regimes for it to explore.

As discussed by Angelopoulos et al. (2013) for bursty bulk flows and reconnection fronts and by Biernat et al. (1987) for flux transfer events, reconnection is often unsteady. While MMS is designed to make rapid plasma and field measurements within moving reconnection sites, its capabilities will apply equally well to the unsteady or time-varying reconnection. In fact, having multiple spacecraft will help in telling the difference between moving and time-varying reconnection regions.

3 Measurement Requirements

The dissipative processes that occur in the reconnection diffusion region can be expressed by the electron momentum equation or generalized Ohm's Law (Vasyliunas 1975):

$$E + v \times B = \eta J + \frac{J \times B}{en} + \frac{\nabla \cdot \vec{P}_e}{en} + \frac{m_e}{e} \frac{dv_e}{dt}. \quad (1)$$

In Eq. (1), E and B are the vector electric and magnetic field, respectively; J is the vector current; v is the plasma velocity; η is anomalous resistivity; P_e is the electron pressure tensor; m_e is electron mass; and n is the plasma density.

Ideal MHD physics will occur if the right-hand side of (1) is zero. If any of the terms are non-zero then MHD will be violated and reconnection can occur. Each of the four terms describes specific physical phenomena to be explored and quantified by the MMS mission and so each term placed certain measurement requirements on the MMS instrumentation. The four terms represent anomalous resistivity, Hall-MHD, divergence of the electron pressure tensor, and electron inertia effects.

Anomalous Resistivity ($E = J$) Ohmic dissipation can occur in a current-carrying collisionless plasma if wave turbulence creates an anomalous resistivity (η). Within a reconnection diffusion region such resistivity can dissipate magnetic-field energy with the inflow and outflow driven by Alfvén waves as described by Parker (1957). The resulting reconnection rates from dominant wave modes are thought to be too slow to be important in explosive reconnection but could be important for the slow-build-up of reconnection (Cassak et al. 2005). Anomalous resistivity is observed to occur in reconnection regions, particularly in association with electron beams produced by reconnection and in connection with observed electron holes (Drake et al. 2003; Fox et al. 2012). One possibility allowed by these results is that the anomalous resistivity may be a result of reconnection rather than its cause. Phenomena suggested as sources of anomalous resistivity include ion-electron streaming instabilities (Vasyliunas 1975; Coppi and Friedland 1971) and the lower hybrid drift instability (Huba et al. 1977). Although wave turbulence is often observed near reconnection regions, the intensity is typically seen to decrease sharply near the center of the neutral sheets where reconnection occurs (e.g., Petkaki et al. 2006). To investigate these effects MMS will measure electromagnetic waves at 0.1 to 5 kHz (encompassing the frequency range of whistler waves) and plasma distribution functions in order to determine which instabilities may be responsible for anomalous resistivity (Torbert et al. 2014; Pollock 2015, this issue). The predicted scale size for the ion-electron streaming instabilities is 20 nT/B \sim 13 km (Coppi and Friedland 1971).

Hall-MHD ($E = J \times B/en$) The Lorentz force causes relative motion between ions and electrons, which produces currents that circulate in the ion diffusion region thereby generating a quadrupolar magnetic field component perpendicular to the plane of reconnection (Sonnerup 1979). This first-level modification to MHD has been described by Huba (1995), who notes its importance to plasma dynamics occurring on length scales less than an ion inertial length (c/ω_{pi}), where c is the speed of light and ω_{pi} the ion plasma frequency, and time scales shorter than an ion cyclotron period. Predictions of Hall-MHD for reconnection have been confirmed in the laboratory and in space (Ren et al. 2005; Borg et al. 2005). As shown by Mandt et al. (1994), whistler-mode waves generated by the Hall currents ultimately carry magnetic field lines away from the ion diffusion region and in this way control the reconnection rate. This idea, that the reconnection rate is determined by phenomena in the ion diffusion region, has been proposed by others as well (e.g., Biskamp et al. 1995). For further progress in Hall-MHD reconnection, MMS must make the following measurements at the ion inertial length scale (~ 250 km in the outer magnetosphere): Magnetic field vector with 0.1-nT resolution, E_{perp} (0 to 10 mV/m), full electron and ion distribution functions, ion flow velocities (100–1000 km/s) with composition (H^+ and O^+), electron cyclotron waves from 0.1 to 6 kHz, and energetic electrons and ions ($\omega/\text{composition}$) with energies up to 500 keV.

Divergence of Electron Pressure Tensor ($E = -\nabla \cdot \vec{P}/en$) The expected role of a divergence of the electron pressure tensor and the associated electron nongyrotropy in electron demagnetization leading to magnetic reconnection is discussed by Hesse et al. (2014). Henderson et al. (2006) have reported measurements of electron pressure tensor gradients using the four Cluster spacecraft. Their results showed that the components of the resulting electric fields normal to the neutral sheet were directed away from the neutral sheet while the Hall electric field components derived from the measured currents were directed toward the neutral sheet. The reconnection electric field itself was not detected, presumably because the electron inertial length is much smaller than the Cluster spacecraft separations. The presence of electron pressure tensor divergence produces ambipolar electric fields and kinetic Alfvén waves along with a transition from Alfvén wave driven reconnection to whistler mode forcing of magnetic field slippage with respect to the electrons (Mandt et al. 1994). For MMS to conduct a definitive test of the importance of the electron pressure tensor divergence to reconnection it must make the following measurements at the scale of the effective ion Larmor radius (~ 20 km) (Vasyliunas 1975; Scudder 1997): full electron distribution functions, vector electric field, electric and magnetic wave components up to several kHz.

Electron Inertia Effects ($E = (m_e/e)dv_e/dt$) At the smallest plasma scales slippage between electrons and the magnetic field is attributed to the non-instantaneous response of thermal electrons to electric field fluctuations, possibly as a result of Langmuir oscillations or other wave-particle interactions. At these scales kinetic Alfvén waves evolve into inertial Alfvén waves, which are dissipated by differential electron motion. An important result of this dissipation is an electric field parallel to B , which is one component of the reconnection electric field. In fact several simulation studies have demonstrated the importance of bulk electron inertia in supporting the reconnection electric field (e.g., Hesse et al. 2004; Ricci et al. 2004; Pritchett 2005). The spatial scale of the phenomena driven by electron inertia is the electron inertial length (c/ω_{pe}), which in the outer magnetosphere is on the order of a few km. Investigation of electron inertial effects places the following measurement requirements on MMS: full electron distribution functions within the electron diffusion region, vector E field, J_{par} , plasma waves up to a few kHz.

The required time scales of the MMS measurements derive from the scale sizes of the electron and ion inertial lengths or skin depths. Equally important are the motions of the reconnection layers and the associated diffusion regions, which have velocities on the order of tens of km/s to over 100 km/s. This motion is generally oscillatory (in and out) at the dayside magnetopause and tailward in the magnetotail. For example, a 5-km wide diffusion region moving at 50 km/s would only contain one of the MMS spacecraft for 0.1 s. Considerations such as this one are what led to the conclusion that full electron distribution functions need to be measured at an unprecedented time resolution of 0.03 s, thereby allowing for at least three measurements during one transit of the diffusion region. Similar considerations applied to ion diffusion regions with characteristic dimensions of 250 km led to the choice of 0.15 s time resolution for ions, thus allowing up to 30 measurements within a moving ion diffusion region.

Previous magnetospheric missions have typically used the rotation of the spacecraft to acquire 3D particle distributions using instruments with 2D fan acceptance angles. Particle measurements on Cluster, for example, are acquired at time resolutions of 2 s (for electrons) and 4 s (for ions) using this method. A new approach had to be devised for MMS, which involves the use of multiple sensors, each of which uses electrostatic scanning of the FOV as was done previously for instruments on the Rosetta (Burch et al. 2007) and Wind (Lin et al. 1995) spacecraft. Eight sensors each for ions and electrons with fields-of-view of $45 \times 180^\circ$ are used to cover 4π steradians in four azimuthal angular steps in 30 ms for electrons and 150 ms for ions (Pollock 2015, this issue).

4 Mission Requirements

In order to accomplish its goals, the MMS spacecraft must sample the most likely reconnection sites repeatedly and probe regions in which the magnetic fields are very nearly antiparallel (which is usually the case in the tail) as well as regions where a significant guide field exists (which is generally true at the dayside boundary). Next, since the reconnection regions are generally moving rapidly (sunward and earthward on the dayside and tailward on the nightside), the spacecraft need to hover in these regions, which is accomplished by placing their orbit apogees near the expected reconnection sites— $12R_E$ on the day side and $25R_E$ on the night side. Two different and highly eccentric orbits are needed to satisfy these requirements. Simplified sketches of these two orbits, one each for mission phases 1 and 2, are shown in Fig. 3. More details about the orbits and phases are provided by Fuselier et al. (2014).

Once near reconnection regions, the four spacecraft will identify them first by sampling the two zones of inflow and outflow, respectively. By subsequently reducing the distances between satellites, ion diffusion regions and then the electron diffusion regions can be sampled in detail. The directions and intensities of currents, electric and magnetic fields, and plasmas and accelerated particles all need to be determined in order to identify the physical processes responsible for reconnection of the magnetic field.

In sunlight, spacecraft continuously emit photoelectrons that tend to charge them up to a positive voltage that can reach up to several tens of volts. This voltage interferes with low-energy plasma measurements and also with the electric-field measurements. MMS will use an Active Spacecraft Potential Control device (ASPOC), which emits indium ions to neutralize the photoelectron current and keep the spacecraft from charging to more than four volts positive (Torkar et al. 2014).

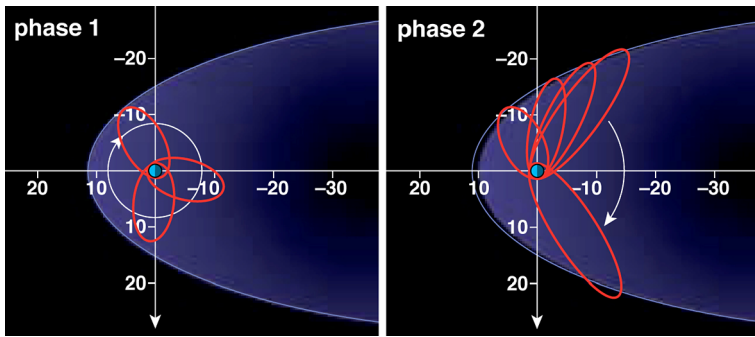


Fig. 3 Simplified sketch in the ecliptic plane of the MMS orbits for Phases 1 and 2

Because physical processes in the ion diffusion region depend sensitively on ion mass, MMS includes a new-generation Hot Plasma Composition Analyzer (HPCA) (Burch et al. 2005; Young et al. 2014), which corrects problems with high proton fluxes that have prevented accurate ion-composition measurements near the dayside magnetospheric boundary (Phan et al. 2003).

MMS includes a comprehensive theory and modeling team that has provided the inputs required for an optimum experiment (Hesse et al. 2014). As described in the Appendix, the SMART team is significantly augmented by the addition of three Interdisciplinary Scientist Teams (Goldstein et al. 2015; Phan et al. 2014; Goldman et al. 2015), which have provided important inputs by virtue of MHD and kinetic modeling and experience with previous multi-spacecraft magnetospheric missions (Cluster and THEMIS).

A major issue is that MMS will make very high rate measurements that will exceed by far the available downlink capacity. For this reason, theory and modeling have been used to design a system that is able to evaluate data quality in near real time and select the most promising intervals for full downlink. This system will be implemented by a large (96 GB), on-board computer memory and the capability to select intervals for downlink based on both the software's sampling of the highest-rate data and the evaluation of lower-rate data by scientists on the ground (Baker et al. 2015).

5 Instrument Descriptions

The instruments carried by each MMS spacecraft are listed in Table 1 along with the basic physical parameters measured and the responsible Co-Investigator and institution. Also listed in Table 1 is the SOC (Science Operations Center). Details of these mission elements are provided in other papers in this issue (Torbert et al. 2014; Ergun 2014; Russell et al. 2014; Lindqvist et al. 2014; Pollock 2015; Mauk et al. 2014; Blake 2015; Young et al. 2014; Torkar et al. 2014). The arrangement of the scientific payload of each spacecraft is shown in Fig. 4. All of the instruments communicate with the spacecraft through the Central Instrument Data Processor (CIDP), which collects and stores telemetry from each instrument and sends it to the spacecraft for downlink. The CIDP provides time and spin synchronization as well as switched power services to the instruments, and forward commands received from the spacecraft flight computer. The integrated MMS observatories are described by Tooley et al. (2015).

Table 1 Major instrument suite elements and responsible co-investigators

FIELDS—3D Electric and magnetic (E , B) fields at <1 ms timing resolution (DC) and waves to 6 kHz (B) and 100 kHz (E). Roy Torbert—UNH

Fast Plasma—Image full sky at 32 energies (10 eV–30 keV): electrons in 30 ms, ions in 150 ms. (n , T , f_e , f_i). *Craig Pollock—GSFC*

Energetic Particles—All-sky viewing of ion and electron energetic particles (20–500 keV) ω /composition (f_e, f_i). Barry Mauk—APL

HPCA—Composition-resolved 3D ion energy distributions (f_i) of H^+ , He^{++} , He^+ , and O^+ (1 eV–40 keV). *Stephen Fuselier*—*SwRI*

ASPOC—Maintains s/c potential to ≤ 4 V. Enables valid (f_i, f_e, E, B) data. *Rumi Nakamura—IWF (Austria)*

SOC—Responsible for instrument operations, data management and archival of science data. *Dan Baker*—*LASP*

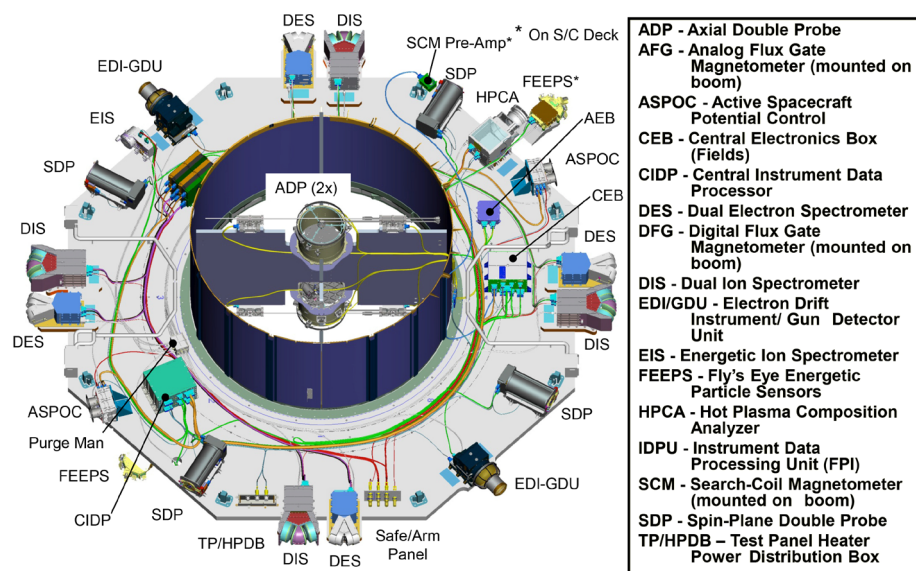


Fig. 4 MMS instrument deck layout

6 Mission Operations

MMS mission operations are described in some detail by Fuselier et al. (2014). In addition to special calibration modes, the instruments basically have two operational modes—slow survey and fast-survey (during which burst data are collected). In the regions of interest ($R > 9R_E$ on the day side and downtail distance $> 15R_E$ on the night side), all instruments operate at their maximum speed (burst data are collected). These regions of interest are chosen as orbital segments along which we have a significant chance of traversing the predicted reconnection zones (the boxes in Fig. 1).

Throughout the regions of interest the four MMS spacecraft are maintained in a tetrahedral or pyramid-shaped configuration, e.g., with one spacecraft at the origin of a carte-

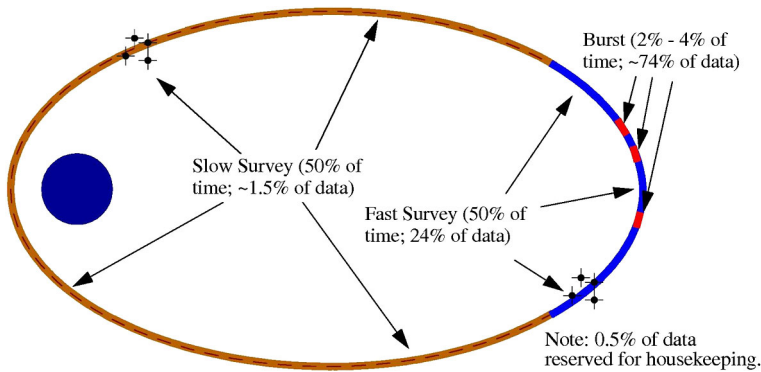


Fig. 5 Ecliptic-plane sketch of MMS orbit showing region of interest in blue ($R > 9R_E$ on the day side and downtail distance of $>15R_E$ on the night side) and burst data intervals in red

sian coordinate system and one spacecraft each along the x , y , and z axis. This formation, which is a tetrahedron, then allows the measurement of the three spatial gradients of various plasma and field parameters. For example, within a uniform region of space these gradients can be used to solve Maxwell's equations for quantities such as current (from $\text{curl } B$) and dB/dt (from $\text{curl } E$) along with vorticity (from $\text{curl } v$), and parallel electric field contributions (from divergence of the electron pressure tensor) (Henderson et al. 2006).

Choice of the size of the tetrahedron, along with the time resolution of the measurements, is made based on the size of the electron and ion diffusion regions and their motions and is limited by engineering and safety constraints. As noted above, the time resolution of the Fast Plasma Instrument is sufficient to resolve the electron and ion inertial lengths even if the reconnection layer is moving over the spacecraft at some tens of km/s. It would also be desirable to set the spacecraft spacing within the inertial length, $5.31(n_e)^{-1/2}$ km for electrons and $210(n_i/m_i)^{-1/2}$ km for ions with n_e and n_i in cm^{-3} and m_i in amu. Estimates for the electron and ion inertial lengths at the magnetopause are <5 km and <200 km, respectively, and because of the lower densities in the magnetotail, these lengths become larger for mission Phase 2. The range of spacecraft separation available to MMS will be 10 km to 400 km. A lower range (10–160 km) will be used on the dayside while a higher range (30–400 km) will be used on the night side. The MMS Flight Dynamics team constantly balances fuel conservation against the mission requirement that high-quality tetrahedrons be maintained throughout the regions of interest. The definition of a high-quality tetrahedron is one in which the ratio of the volume to the theoretical volume of a regular tetrahedron of the same size is at least 0.8. Further details on spacecraft spacing and its management during the mission are provided by Fuselier et al. (2014).

A particular challenge for MMS is the fact that the S-band data downlink system can only return 4 gigabits of data per spacecraft per day through the Deep Space Network (DSN). At this rate only about 20 minutes of burst-mode data can be downloaded per day. For the rest of the day the burst-mode data, which are acquired in the regions of interest, have to be averaged down to a fast-survey rate for transmission. The segmentation among slow-survey, fast-survey and burst-mode data is illustrated in Fig. 5. More detailed descriptions are provided by Fuselier et al. (2014) and Baker et al. (2015). Fast-survey data have time resolutions typical of previous magnetospheric missions, e.g., 4.5 s for full 3D plasma distributions. In order to insure that the best burst data are chosen for transmission, the CIDP contains a 96-GB memory, which is sufficient to hold up to three days of full resolution data. During

Table 2 Top level burst-mode parameters

Physical signature	Trigger parameter
Reconnection jets	Ion flow reversals
Magnetopause and neutral sheet detection	Large B variations
Large flows surrounding reconnection sites	Large E
Magnetopause and neutral sheet detection	Large electron currents
Particle acceleration produced by reconnection	Electron and ion beams
Electron diffusion region	E parallel to B

passage through the regions of interest, each instrument automatically interrogates its data and assigns quality factors to each 10-s segment. Table 2 shows a top-level description of the types of signatures that are of interest to each instrument with details provided by Fuselier et al. (2014). The quality factors for all the instruments on a single spacecraft are combined on board to generate spacecraft data quality indices, which are transmitted along with the survey data. In the SOC the quality indices for the four spacecraft are combined into a mission quality index. The burst-mode data are held on board to allow a Scientist-in-the-Loop (SITL) to examine the fast survey data and the burst quality indices to validate whether the on-board system chose the best intervals. If not, the SITL scientist can change the burst data downlink priorities. The combination of on-board and SITL burst-data collection processes will be used throughout the mission or until one system proves to be the most reliable. The main advantage of the on-board system is that it acts without bias on the burst-mode trigger data. The SITL also has access to this trigger data information and, depending on downlink schedules, will have access to fast-survey quicklook data to add to their personal experience with plasma boundary identification along with a larger-scale view of the plasma environment, which should at times prove to be advantageous.

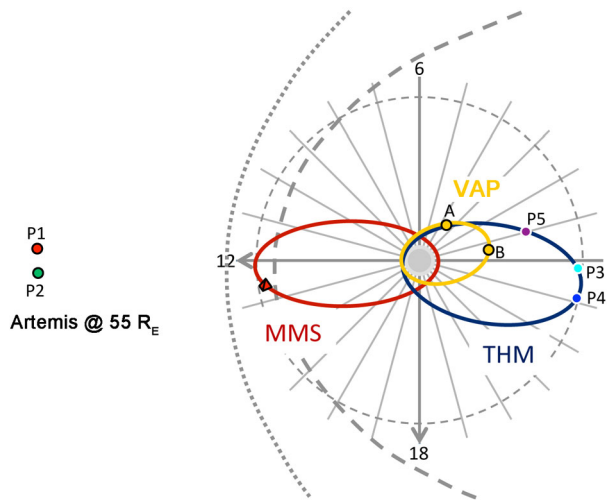
7 Data Products

The MMS mission will have a completely open data system with no proprietary data periods. The primary data set will reside in the MMS Science Data Center (SDC) (Baker et al. 2015). The SDC, along with the Payload Operations Center (POC) make up the MMS Science Operations Center (SOC), which resides at the Laboratory for Atmospheric and Space Physics (LASP) at the University of Colorado. QuickLook science data will be available on-line within 24 hours of their acquisition, and, after an initial 6-month period of operational check-out and validation, calibrated Level-2 data will be provided to the SOC by the instrument teams within 30 days of receipt for use by the science community. Level-3 or mission-level data will be produced on an event basis and provided on-line as it is generated. A comprehensive description of the various MMS data products is provided by Baker et al. (2015).

8 Summary and Conclusions

MMS is a strategic heliophysics mission, which was developed as part of the NASA Solar-Terrestrial Probes (STP) program as the fourth mission following TIMED, Solar-B (Hinode), and STEREO. The purpose of STP is to conduct fundamental science investigations

Fig. 6 Elements of the Heliophysics System Observatory most connected to MMS (Van Allen Probes and THEMIS)



that form the basis for focused research conducted by the Living With a Star (LWS) Program. LWS missions target the linkages across the interconnected system that emphasize the science necessary to understand those aspects of the Sun and space environment that most directly affect life and society. The first two LWS missions are the Solar Dynamics Observatory (SDO) and the Van Allen Probes (formerly the Radiation Belt Storm Probes).

MMS is especially appropriate to the STP program in that it investigates a fundamental physical process, magnetic reconnection, that occurs throughout the universe, in space as well as in plasma laboratories. The magnetosphere is to some extent incidental to the study of reconnection but is crucial because it is the only accessible laboratory in space for detailed study of this important phenomenon. However, the MMS data will provide significant data elements to the NASA Heliophysics Observatory (HSO), which uses a combination of focused science missions to achieve a global view of geospace. A sketch of the segment of the HSO most connected to MMS is shown in Fig. 6. In the time period of MMS, especially valuable conjunctions are anticipated with the THEMIS and Van Allen Probes missions. In order to achieve conjunctions, specific maneuvers of THEMIS were made well in advance of the MMS launch. In addition to the configuration shown in Fig. 6, times when THEMIS is in the near tail and Artemis is in the deep tail will be especially valuable as shown in the study by Angelopoulos et al. (2013).

MMS significantly advances the state of the art in instrumentation, data acquisition and spacecraft navigation. It will make major advances in the rapidly expanding field of magnetic reconnection research. Its payload is specifically designed to investigate dynamic phenomena at the electron temporal and spatial scales and make more accurate 3D electric and magnetic field and ion composition measurements than have previously been performed. A particularly notable achievement was to obtain full-sky measurements of suprathermal electrons and ions at dramatically finer time scales (30 ms for electrons and 150 ms for ions).

The advances in measurement time scales led to a very high on-board data rate of which only a small fraction ($\sim 2\%$) will be transmitted to the ground by the S-band telemetry system. A two-pronged system for selecting the most scientifically valuable high-rate data was devised. It consists of an on-board data assessment system and a ground-based scientist-in-the-loop system, which checks on and improves the data selection by the on-board system.

The requirement to perform experiments at the electron scale also demanded the ability to navigate the four MMS spacecraft to separations at small as 10 km with an accuracy of 100 m while maintaining a spatial configuration that approximates a regular tetrahedron to 80 % accuracy within the scientific regions of interest. This configuration allows for accurate determination of the spatial gradients of relevant plasma and field quantities such as vector electric and magnetic fields and plasma densities and pressure tensors.

The measurement requirements for MMS were derived from numerical models of the reconnection process and from the experimental results of previous missions. During the extended period of development (almost ten years from the final selection to launch) rapid advances in magnetic reconnection research have been made, particularly the experimental results at the MHD and ion scales by the ESA Cluster mission and the development of 3D kinetic simulations. Nonetheless, the electron-scale physics that controls the reconnection of magnetic fields is still as mysterious as ever. The fact that the MMS measurements were designed to probe the plasmas at their smallest scale has led to the ability of MMS to perform a definitive experiment on magnetic reconnection. The expectation is that MMS will help solve the reconnection problem by answering all of the outstanding questions that can currently be posed.

Acknowledgements The dedicated efforts of the entire MMS team are greatly appreciated. We are especially grateful to the leadership of the GSFC Project Manager, Craig Tooley, his Deputy, Brent Robertson, and the SwRI SMART Project Manager, Ron Black. This work was supported by NASA Contract No. NNG04EB99C at SwRI.

Open Access This article is distributed under the terms of the Creative Commons Attribution 4.0 International License (<http://creativecommons.org/licenses/by/4.0/>), which permits unrestricted use, distribution, and reproduction in any medium, provided you give appropriate credit to the original author(s) and the source, provide a link to the Creative Commons license, and indicate if changes were made.

Appendix

A.1 Brief History of Magnetospheric Multiscale

The MMS mission officially began on May 20, 2002 with the release of a NASA Formulation Authorization, which provided for a suite of instruments consistent with that described in the STDT report to be flown on a constellation of at least four identically instrumented, spinning, partially redundant, spacecraft placed into an elliptical orbit. The MMS mission design life was set at two years. As part of the STP program, responsibility was delegated to the Goddard Space Flight Center (GSFC) as the Lead Center.

Because of the need for maximum congruence and simultaneity of the measurements the MMS Announcement of Opportunity (AO), issued in December 2002, solicited a single instrument suite science team under the leadership of a single Principal Investigator (PI). This PI would provide the four science payloads and partner with NASA to design, build, and operate the mission. In May 2005 NASA selected the "Solving Magnetospheric Acceleration, Reconnection, and Turbulence (SMART)," team led by Southwest Research Institute to work with the Goddard Space Flight Center for the full cycle of mission formulation and development. Working cooperatively, GSFC and the SMART team finalized the MMS Program Level Requirements on November 14, 2007 and the mission moved steadily forward toward its successful launch on March 12, 2015.

In February 2008, during the development phase of the mission, NASA selected three Interdisciplinary Science (IDS) investigations on ten-year grants to work synergistically and

cooperatively with the SMART science team as part of the MMS Science Working Group for implementation and successful completion of the mission.

References

- V. Angelopoulos et al., Electromagnetic energy conversion at reconnection fronts. *Science* **341**, 1478–1482 (2013). doi:[10.1126/science.1236992](https://doi.org/10.1126/science.1236992)
- D.N. Baker et al., Magnetospheric multiscale instrument suite operations and data system. *Space Sci. Rev.* (2015). doi:[10.1007/s11214-014-0128-5](https://doi.org/10.1007/s11214-014-0128-5)
- H.K. Biernat et al., Unsteady Petschek reconnection. *J. Geophys. Res.* **92**, 3392–3396 (1987). doi:[10.1029/JA092iA04p03392](https://doi.org/10.1029/JA092iA04p03392)
- D. Biskamp, J.F. Drake, E. Schwarz, Ion-controlled collisionless magnetic reconnection. *Phys. Rev. Lett.* **75**, 3850–3853 (1995). doi:[10.1103/PhysRevLett.75.3850](https://doi.org/10.1103/PhysRevLett.75.3850)
- J.B. Blake, The Fly’s Eye Energetic Particle Spectrometer (FEEPS) sensors for the Magnetospheric Multiscale (MMS) mission. *Space Sci. Rev.* (2015, in press). doi:[10.1007/s11214-015-0163-x](https://doi.org/10.1007/s11214-015-0163-x)
- A.L. Borg et al., Cluster encounter of a magnetic reconnection diffusion region in the near-Earth magnetotail on September 19, 2003. *Geophys. Res. Lett.* **32**, L19105 (2005). doi:[10.1029/2005GL023794](https://doi.org/10.1029/2005GL023794)
- J.L. Burch, J.F. Drake, Reconnecting magnetic fields. *Am. Sci.* **97**, 392–399 (2009)
- J.L. Burch et al., Technique for increasing dynamic range of space-borne ion composition instruments. *Rev. Sci. Instrum.* **76**, 103301 (2005)
- J.L. Burch et al., RPC-IES: the ion and electron sensor of the Rosetta Plasma Consortium. *Space Sci. Rev.* **128**, 697–712 (2007). doi:[10.1007/s11214-006-9002-4](https://doi.org/10.1007/s11214-006-9002-4)
- H.V. Cain, I.G. Richardson, O.C. St. Cyr, Coronal mass ejections, interplanetary ejecta and geomagnetic storms. *Geophys. Res. Lett.* **27**, 3591–3594 (2000)
- P.A. Cassak, M.A. Shay, Magnetic reconnection for coronal conditions: reconnection rates, secondary islands and onset. *Space Sci. Rev.* **172**, 283–302 (2012). doi:[10.1007/s11214-011-9755-2](https://doi.org/10.1007/s11214-011-9755-2)
- P.A. Cassak, M.A. Shay, J.F. Drake, Catastrophe model for fast magnetic reconnection onset. *Phys. Rev. Lett.* **95** 235002 (2005). doi:[10.1103/PhysRevLett.95.235002](https://doi.org/10.1103/PhysRevLett.95.235002)
- B. Coppi, A.B. Friedland, Processes of magnetic-energy conversion and solar flares. *Astrophys. J.* **169**, 379–404 (1971)
- S. Curtis, The Magnetospheric Multiscale Mission—Resolving Fundamental Processes in Space Plasmas. Report of the NASA Science and Technology Definition Team for the Magnetospheric Multiscale. (MMS) Mission (NASA/TM; 2000-209883) (1999)
- G.A. Doschek, D.E. McKenzie, H.P. Warren, Plasma dynamics above solar flare soft X-ray loop tops. *Astrophys. J.* **788**, 26 (2014). doi:[10.1088/0004-637X/788/1/26](https://doi.org/10.1088/0004-637X/788/1/26)
- J. Drake, M. Swisdak, C. Cattell, M. Shay, B. Rogers, A. Zeiler, Formation of electron holes and particle energization during magnetic reconnection. *Science* **299**, 873 (2003)
- J.F. Drake et al., Ion heating resulting from pickup in magnetic reconnection exhausts. *J. Geophys. Res.* **114**, A05111 (2009). doi:[10.1029/2008JA013701](https://doi.org/10.1029/2008JA013701)
- J.W. Dungey, Interplanetary magnetic field and the auroral zones. *Phys. Rev. Lett.* **6**, 47–48 (1961). doi:[10.1103/PhysRevLett.6.47](https://doi.org/10.1103/PhysRevLett.6.47)
- R.E. Ergun, The axial double probe and fields signal processing for the MMS mission. *Space Sci. Rev.* (2014). doi:[10.1007/s11214-014-0115-x](https://doi.org/10.1007/s11214-014-0115-x)
- W. Fox, M. Porkolab, J. Egedal, N. Katz, A. Le, Observations of electron phase-space holes driven during magnetic reconnection in a laboratory plasma. *Phys. Plasmas* **19**, 032118 (2012)
- S.A. Fuselier et al., Magnetospheric multiscale science mission profile and operations. *Space Sci. Rev.* (2014). doi:[10.1007/s11214-014-0087-x](https://doi.org/10.1007/s11214-014-0087-x)
- A.A. Galeev, R. Rosner, G.S. Vaiana, Structured coronae of accretion disks. *Astrophys. J.* **229**, 318–326 (1979)
- R.G. Giovanelli, Magnetic and electric phenomena in the Sun’s atmosphere associated with sunspots. *Mon. Not. R. Astron. Soc.* **107**, 338 (1947)
- C.P. Goff et al., A slow coronal mass ejection with rising X-ray source. *Astron. Astrophys.* **434**, 761–771 (2005). doi:[10.1051/0004-6361:20042321](https://doi.org/10.1051/0004-6361:20042321)
- M. Goldman et al., What can we learn about magnetotail reconnection from 2D PIC Harris-sheet simulations? *Space Sci. Rev.* (2015)
- M. Goldstein et al., Mission oriented support and theory (MOST) for MMS—the Goddard Space Flight Center/University of California Los Angeles interdisciplinary science program. *Space Sci. Rev.* (2015). doi:[10.1007/s11214-014-0127-6](https://doi.org/10.1007/s11214-014-0127-6)

- J.T. Gosling, M.F. Thomsen, S.J. Bame, Accelerated plasma flows at the near-tail magnetopause. *J. Geophys. Res.* **91**, 3029–3041 (1986)
- D.B. Graham et al., Electron dynamics in the diffusion region of an asymmetric magnetic reconnection. *Phys. Rev. Lett.* **112**, 215004 (2014). doi:[10.1103/PhysRevLett.112.215004](https://doi.org/10.1103/PhysRevLett.112.215004)
- P.D. Henderson et al., Cluster PEACE observations of electron pressure tensor divergence in the magnetotail. *Geophys. Res. Lett.* **33**, L22106 (2006). doi:[10.1029/2006GL027868](https://doi.org/10.1029/2006GL027868)
- M. Hesse, M. Kuznetsova, J. Birn, The role of electron heat flux in guide-field magnetic reconnection. *Phys. Plasmas* **11**, 5387 (2004)
- M. Hesse et al., Theory and modeling for the Magnetospheric Multiscale mission. *Space Sci. Rev.* (2014). doi:[10.1007/s11214-014-0078-y](https://doi.org/10.1007/s11214-014-0078-y)
- F. Hoyle, *Some Recent Researches in Solar Physics* (Cambridge University Press, Cambridge, 1949)
- J.D. Huba, Hall magnetohydrodynamics in space and laboratory plasmas. *Phys. Plasmas* **2**, 2504–2513 (1995)
- J.D. Huba et al., The lower-hybrid-drift instability as a source of anomalous resistivity for magnetic field reconnection. *Geophys. Res. Lett.* **4**, 125 (1977)
- H. Ji et al., Magnetic reconnection with Sweet-Parker characteristics in two-dimensional laboratory plasmas. *Phys. Plasmas* **6**, 1743 (1999)
- O. Le Contel et al., The search-coil magnetometer for MMS. *Space Sci. Rev.* (2014). doi:[10.1007/s11214-014-0096-9](https://doi.org/10.1007/s11214-014-0096-9)
- R.H. Levy, H.E. Petschek, G.L. Siscoe, Aerodynamic aspects of the magnetospheric flow. *AIAA J.* **2**, 2065–2076 (1964)
- R.P. Lin et al., A three-dimensional plasma and energetic particle investigation for the wind spacecraft. *Space Sci. Rev.* **71**, 125–153 (1995)
- P.-A. Lindqvist et al., The spin-plane double probe electric field instrument for MMS. *Space Sci. Rev.* (2014). doi:[10.1007/s11214-014-0116-9](https://doi.org/10.1007/s11214-014-0116-9)
- Y.E. Litvinenko, J. Chae, Signatures of Sweet-Parker magnetic reconnection in the solar chromosphere. *Astron. Astrophys.* **495**, 953–957 (2009). doi:[10.1051/0004-6361/200811034](https://doi.org/10.1051/0004-6361/200811034)
- M.E. Mandt, R.E. Denton, J.F. Drake, Transition to whistler mediated magnetic reconnection. *Geophys. Res. Lett.* **21**, 73–76 (1994)
- B.H. Mauk et al., The Energetic Particle Detector (EPD) Investigation and the Energetic Ion Spectrometer (EIS) for the Magnetospheric Multiscale (MMS) mission. *Space Sci. Rev.* (2014). doi:[10.1007/s11214-014-0055-5](https://doi.org/10.1007/s11214-014-0055-5)
- D.E. McKenzie, Turbulent dynamics in solar flare sheet structures measured with local correlation tracking. *Astrophys. J.* **766**, 39 (2013). doi:[10.1088/0004-637X/766/1/39](https://doi.org/10.1088/0004-637X/766/1/39)
- F.S. Mozer, P.L. Pritchett, Regions associated with electron physics in asymmetric magnetic field reconnection. *Geophys. Res. Lett.* **36**, L07102 (2009). doi:[10.1029/2009GL037463](https://doi.org/10.1029/2009GL037463)
- F.S. Mozer, M. Wilber, J.F. Drake, Wave associated anomalous drag during magnetic field reconnection. *Phys. Plasmas* **18**, 102902 (2011). doi:[10.1063/1.3647508](https://doi.org/10.1063/1.3647508)
- T. Nagai et al., Three-dimensional structure of magnetic reconnection in the magnetotail from Geotail observations. *J. Geophys. Res.* **118**, 1667–1678 (2013). doi:[10.1002/jgra.50247](https://doi.org/10.1002/jgra.50247)
- E.N. Parker, Sweet's mechanism for merging magnetic fields in conducting fluids. *J. Geophys. Res.* **62**, 509 (1957)
- G. Paschmann et al., Plasma acceleration at the Earth's magnetopause: evidence for reconnection. *Nature* **282**, 243–246 (1979). doi:[10.1038/282243a0](https://doi.org/10.1038/282243a0)
- P. Petkaki, M.P. Freeman, A.P. Walsh, Cluster observations of broadband electromagnetic waves in and around a reconnection region in the Earth's magnetotail current sheet. *Geophys. Res. Lett.* **33**, L16105 (2006). doi:[10.1029/23006GL027066](https://doi.org/10.1029/23006GL027066)
- H.E. Petschek, Magnetic field annihilation, in *AAS-NASA Symposium on the Physics of Solar Flares*. NASA Spec. Publ., vol. SP-50 (1964), p. 425
- H.E. Petschek, The concept of rapid magnetic field reconnection: a retrospective view, in *Physics of the Magnetopause*. Geophysical Monograph, vol. 90, ed. by P. Song, B.U.Ö. Sonnerup, M.F. Thomsen (American Geophysical Union, Washington, 1995)
- T.D. Phan et al., Simultaneous Cluster and IMAGE observations of cusp reconnection and auroral proton spot for northward IMF. *Geophys. Res. Lett.* **30**, 1509 (2003). doi:[10.1029/2003GL016885](https://doi.org/10.1029/2003GL016885)
- T.D. Phan et al., A magnetic reconnection X-line extending more than 390 Earth radii in the solar wind. *Nature* **439**, 175–178 (2006). doi:[10.1038/nature04393](https://doi.org/10.1038/nature04393)
- T.D. Phan et al., Establishing the context for reconnection diffusion region encounters and strategies for the capture and transmission of diffusion region burst data by MMS. *Space Sci. Rev.* (2014). doi:[10.1007/s11214-015-0150-2](https://doi.org/10.1007/s11214-015-0150-2)
- C.J. Pollock, Fast plasma instrument for MMS. *Space Sci. Rev.* (2015, this issue)

- P.L. Pritchett, Onset and saturation of guide-field magnetic reconnection. *Phys. Plasmas* **12**, 062301 (2005). doi:[10.1063/1.1914309](https://doi.org/10.1063/1.1914309)
- Y. Ren et al., Experimental verification of the Hall effect during magnetic reconnection in a laboratory plasma. *Phys. Rev. Lett.* **95**, 055003 (2005)
- J.U. Ricci et al., Collisionless magnetic reconnection in the presence of a guide field. *Phys. Plasmas* **11**, 4102 (2004)
- C.T. Russell et al., The magnetospheric multiscale magnetometers. *Space Sci. Rev.* (2014). doi:[10.1007/s11214-014-0057-3](https://doi.org/10.1007/s11214-014-0057-3)
- J.D. Scudder, Theoretical approaches to the description of magnetic merging: the need for finite β_e , anisotropic, ambipolar Hall MHD. *Space Sci. Rev.* **80**, 235–267 (1997). doi:[10.1023/A:1004978021644](https://doi.org/10.1023/A:1004978021644)
- B.U.Ö. Sonnerup, Magnetic field reconnection, in *Solar System Plasma Physics*, vol. III, ed. by L.J. Lanzerotti, C.F. Kennel, E.N. Parker (North-Holland, Amsterdam, 1979), pp. 45–108
- P.A. Sweet, The neutral point theory of solar flares, in *Proceedings of the International Astronomical Union Symposium on Electromagnetic Phenomena in Cosmical Physics University (No. 6, Stockholm, 1956)* (Cambridge Press, Cambridge, 1958), p. 123
- C.R. Tooley et al., The MMS observatory. *Space Science Rev.* (2015)
- R.B. Torbert et al., The FIELDS Instrument Suite on MMS: Scientific objectives, measurements, and data products. *Space Sci. Rev.* (2014). doi:[10.1007/s11214-014-0109-8](https://doi.org/10.1007/s11214-014-0109-8)
- K. Torkar et al., Active spacecraft potential control investigation. *Space Sci. Rev.* (2014, this issue). doi:[10.1007/s11214-014-0049-3](https://doi.org/10.1007/s11214-014-0049-3)
- D.A. Uzdensky, R.M. Kulsrud, Physical origin of the quadrupole out-of-plane magnetic field in Hall magnetohydrodynamic reconnection. *Phys. Plasmas* **13**, 062305 (2006). doi:[10.1063/1.2209627](https://doi.org/10.1063/1.2209627)
- V.M. Vasyliunas, Magnetic field line merging. *Rev. Geophys. Space Phys.* **13**, 303–336 (1975)
- D.F. Webb et al., The relationship of halo CMEs, magnetic clouds and magnetic storms. *J. Geophys. Res.* **105**, 7491 (2000)
- M. Yamada et al., Study of driven magnetic reconnection in a laboratory plasma. *Phys. Plasmas* **4**, 1936 (1997)
- D.T. Young et al., Hot plasma composition analyzer for the Magnetospheric Multiscale Mission. *Space Sci. Rev.* (2014). doi:[10.1007/s11214-014-0119-6](https://doi.org/10.1007/s11214-014-0119-6)